Earth and Planetary Science Letters 308 (2011) 161–171

Contents lists available at ScienceDirect

Earth and Planetary Science Letters

journal homepage: www.elsevier.com/locate/epsl

# Solar modulation of North Atlantic central Water formation at multidecadal timescales during the late Holocene

Audrey Morley [a,b,*], Michael Schulz [a], Yair Rosenthal [b], Stefan Mulitza [a], André Paul [a], Carsten Rühlemann [c]

[a] MARUM, Center for Marine Environmental Sciences and Faculty of Geosciences, University of Bremen, GEO Building, Klagenfurter Straße, D-28359 Bremen, Germany
[b] Institute for Marine and Coastal Sciences and Department of Earth and Planetary Sciences, Rutgers the State University of New Jersey, 71 Dudley Road, New Brunswick, NJ 08901-8525, USA
[c] Federal Institute for Geosciences and Natural Resources, Stilleweg 2, 30655 Hannover, Germany

ARTICLE INFO

*Article history:*
Received 30 November 2010
Received in revised form 3 May 2011
Accepted 22 May 2011
Available online 14 June 2011

Editor: P. DeMenocal

*Keywords:*
benthic Mg/Ca paleothermometry
North Atlantic central water formation
Late Holocene
solar minima — LIA
NAO
climate signal transfer

ABSTRACT

Understanding natural climate variability in the North Atlantic region is essential not only to assess the sensitivity of atmosphere–ocean climate signal exchange and propagation, but also to help distinguish between natural and anthropogenic climate change. The North Atlantic Oscillation is one of the controlling modes in recent variability of atmosphere–ocean linkages and ice/freshwater fluxes between the Polar and North Atlantic Ocean. Through these processes the NAO influences water mass formation and the strength of the Atlantic Meridional Overturning circulation and thereby variability in ocean heat transport. However, the impact of the NAO as well as other forcing mechanisms on multidecadal timescales such as total solar irradiance on Eastern North Atlantic Central Water production, central water circulation, and climate signal propagation from high to low latitudes in the eastern subpolar and subtropical basins remains uncertain. Here we use a 1200 yr long benthic foraminiferal Mg/Ca based temperature and oxygen isotope record from a ~900 m deep sediment core off northwest Africa to show that atmosphere–ocean interactions in the eastern subpolar gyre are transferred at central water depth into the eastern boundary of the subtropical gyre. Further we link the variability of the NAO (over the past 165 yrs) and solar irradiance (Late Holocene) and their control on subpolar mode water formation to the multidecadal variability observed at mid-depth in the eastern subtropical gyre. Our results show that eastern North Atlantic central waters cooled by up to ~0.8 ± 0.7 °C and densities decreased by $\sigma_\theta = 0.3 \pm 0.2$ during positive NAO years and during minima in solar irradiance during the Late Holocene. The presented records demonstrate the sensitivity of central water formation to enhanced atmospheric forcing and ice/freshwater fluxes into the eastern subpolar gyre and the importance of central water circulation for cross-gyre climate signal propagation during the Late Holocene.


## 1. Introduction

The state of the North Atlantic Oscillation (NAO) in combination with subpolar gyre dynamics (Hatun et al., 2005) determines regional sea surface heat loss and winter convection by modulating both the variability in the westerly wind stress and fresh water budgets in the North Atlantic (Curry and Mauritzen, 2005; Furevik and Nilsen, 2005; Johnson and Gruber, 2007; Marshall et al., 2001a; Marshall et al., 2001b), and thereby, influencing the intensity of the deep overturning branch of the Atlantic Meridional Overturning Circulation (AMOC) in the Nordic and Labrador Seas (Boessenkool et al., 2007; Dickson et al., 2002; Dickson et al., 2000; Eden and Jung, 2001; Hatun et al., 2005; Shindell et al., 2001b). However, the region with the strongest response to NAO-modulated wind-stress is in the subpolar basin south of Iceland, where westerlies are up to 8 m $s^{-1}$ stronger during extremely positive NAO (+) years (Hurrell, 1995) due to the enhanced pressure gradient between the Icelandic Low and Azores High and result, via sea surface heat loss, in sea surface temperatures (SST) several tenths of degrees (~0.7 °C) colder than on average (Furevik and Nilsen, 2005; Johnson and Gruber, 2007). Subpolar Mode Water (SPMW) forms in this region (Fig. 1) via subduction (Tomczak and Godfrey, 1994) and after formation comprise a large fraction of Eastern North Atlantic Central Water (ENACW) (Iselin, 1936; Poole and Tomczak, 1999). A positive NAO phase shift is thus associated with cooler and fresher ENACW (Johnson and Gruber, 2007; Pérez et al., 2000).

The formation, subduction and subsequent southward flow of ENACW at densities between $\sigma_\theta = 27.3$ and 27.6 kg/$m^3$ (Levitus, 1989; McCartney and Talley, 1982), into the STG is well established (Keffer, 1985; Levitus, 1989; McCartney and Talley, 1982; McDowell et al., 1982). ENACW formation and circulation provide therefore a direct link between both gyres and offer the opportunity to investigate the influence of atmospheric–ocean linkages in the

* Corresponding author at: Institute for Marine and Coastal Sciences and Department of Earth and Planetary Sciences, Rutgers the State University of New Jersey, 71 Dudley Road, New Brunswick, NJ 08901-8525, USA. Tel.: +1 732 932 6555; fax: +1 732 932 8578.
*E-mail address:* morley@marine.rutgers.edu (A. Morley).

0012-821X/$ – see front matter © 2011 Elsevier B.V. All rights reserved.
doi:10.1016/j.epsl.2011.05.043

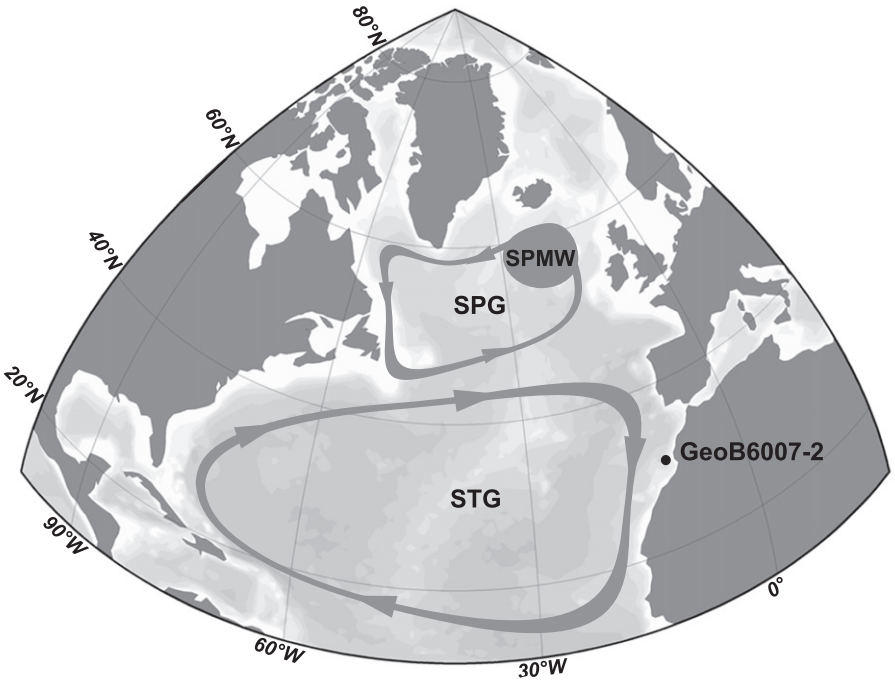


**Fig. 1.** Study area: the location of core GeoB6007-2 (30.85°N, 10.27°W at 899 m depth) marked by a black circle. Simplified SPG and STG positions and circulation patterns are indicated by gray loops modified after Bamberg et al. (2010). The formation region of SPMW is marked by a circle between ~50-63°N east of 25°W (Levitus, 1989; McCartney and Talley, 1982).

subpolar North Atlantic on central water formation and cross gyre climate signal propagation.

In addition to the NAO, recent numerical model simulations (Ammann et al., 2007; Swingedouw et al., 2010) and paleoproxy reconstructions (Knudsen et al., 2009) as well as the re-analysis of published proxy data (Lockwood et al., 2010; Lohmann et al., 2004) provide support for the existence of ocean–atmosphere linkages over the subpolar basin that communicate and amplify relatively small radiative changes in total solar irradiance (ΔTSI) (Lean, 2010; Shindell et al., 2001b) into a climate signal extending beyond the northeastern Atlantic region at multidecadal timescales. The NAO and possibly ΔTSI are thus two important factors controlling recent and long-term variability in atmosphere–ocean linkages over the north Atlantic at multidecadal timescales.

However, the impact of multidecadal variations in NAO mode and ΔTSI on meridional climate signal transfer in the North Atlantic remains uncertain for the Late Holocene. The lack of evidence for past and present records assessing atmospheric and mid-depth ocean linkages is due to the scarcity of high resolution, undisturbed, and well-dated marine records (Sicre et al., 2008), and a focus on SST proxies in the recent literature, rather than proxies for bottom water temperatures (Katz et al., 2010) needed to reconstruct central water properties.

In the present study we investigate oceanic central water connections between mid-depth subpolar and subtropical latitudes. We present a high resolution 1200-yr long paleotemperature and stable isotopic record based on benthic foraminifera collected at 900 m depth from the northwest African continental shelf in the eastern boundary of the STG thus providing new insights into natural mid-depth climate signal propagation. In particular, we discuss two hypotheses on atmospheric mid-depth oceanic linkages and their relationship to NAO and ΔTSI variability at multidecadal timescales. The first hypothesis is that mid-depth cooling in the eastern boundary of the STG is caused by enhanced Ekmann pumping resulting in a shoaling of the local thermocline in conjunction with positive NAO years (Curry and McCartney, 2001). A shoaling at 900 m depth may then allow the incursion of relatively cooler and fresher Antarctic intermediate water (AAIW) to result in colder and fresher mid-depth temperatures in the eastern STG. The second hypothesis proposes that colder mid-depth temperatures in the eastern STG originate from the subpolar gyre and represent the formation of colder SPMW and ENACW during positive NAO years that are subducted and transported underneath the North Atlantic Current into the STG (Keffer, 1985; Levitus, 1989; McCartney and Talley, 1982; McDowell et al., 1982); (Fig. 2).

## 2. Materials and methods

### 2.1. Core location

During METEOR Leg M45 in 1999, gravity core GeoB6007-2 and multicore GeoB6007-1 were collected from the eastern boundary of

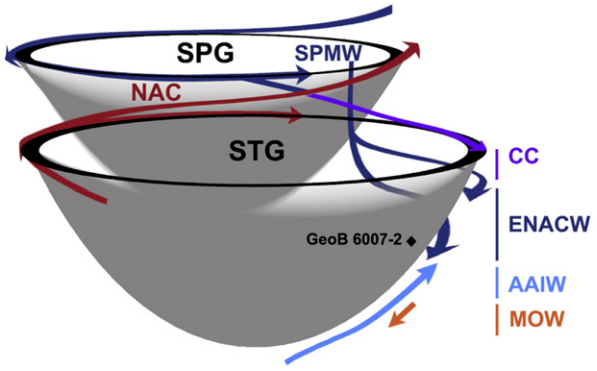


**Fig. 2.** Schematic representation of the formation and cross-gyre transfer of Eastern North Atlantic Central Waters (ENACW) via Subpolar Mode Water (SPMW) formation in the eastern Subpolar gyre (SPG). Also shown are the North Atlantic Current (NAC) and Canary Current as well as Antarctic Intermediate Water (AAIW) and Mediterranean Outflow Water (MOW) present below the core site underneath ENACW.

the STG at 30.85°N, 10.27°W at 899 m water depth (Fig. 1) (Hebbeln et al., 1999). The predominant water mass at the core site is ENACW occupying density surfaces between $\sigma_\theta = 26.6$ and 27.3 kg/m$^3$. At a depth between 900 and 1300 m, a salinity minimum at density ranges of $\sigma_\theta = 27.3$ to 27.6 kg/m$^3$ provides evidence for strongly modified AAIW (Knoll et al., 2002). A salinity maximum at depths below 1300 m and densities exceeding $\sigma_\theta = 27.6$ kg/m$^3$ indicates the presence of Mediterranean outflow water (MOW) (Arhan et al. 1994, Knoll et al. 2002). Modern seasonal and inter-annual variabilities in temperature and salinity are very small at 900 m water depth and there is no indication for changing water masses at the core site on these timescales (Knoll et al. 2002). Modern temperature and salinity values at the core site are of 7.8–7.9 °C and 35.45 psu respectively.

High sedimentation rates at the core location arise from high terrigenous input and extensive perennial local oceanic productivity within the Cape Ghir upwelling filament (Sarnthein et al. 1982, Meggers et al. 2002, Kuhlmann et al. 2004a, Eberwein and Mackensen 2008). As a result accumulation rates range between 70 to 100 cm kyr $^{-1}$ at 900 m depth (Bamberg et al., 2010; Kim et al., 2007; Kuhlmann et al., 2004). GeoB6007-2 and GeoB6007-1 are thus ideally located to investigate high resolution, multi-decadal linkages between SPMW variability and mid-depth STG ventilation.

### 2.2. Paired Mg/Ca–$\delta^{18}O_{sw}$ measurements

We reconstructed central water temperature during the Late Holocene by measuring Mg/Ca and oxygen isotopic values ($\delta^{18}O$) on the benthic foraminifera *Hyalinea balthica*. *H. balthica* is a shallow infaunal benthic foraminifera living within the top 1.5 cm of oxygenated, nutrient rich, fine grained sediments (Schmiedl et al. 2000, Villanueva Guimerans and Cervera Currado, 1999). Off the NW African coast *H. balthica* tests often cluster together with *Bulimina marginata*, a species typically associated with perennially productive areas and high chlorophyll concentrations that indicate a high organic-matter supply (Eberwein and Mackensen 2006). The isotopic oxygen and carbon compositions ($\delta^{18}O$ and $\delta^{13}C$) of the foraminiferal shells were measured at the Stable Isotope Laboratory of the University of Bremen using a Finnigan MAT 251 mass spectrometer equipped with an automatic carbonate preparation device and reported against Vienna PDB (VPDB). Internal precision, based on replicates of a limestone standard, was better than ±0.07‰. Up to 25 (mean: 20 individuals) *H. balthica* tests from the 250–350 μm size fraction were analyzed for Mg/Ca ratios, using a modified reductive, oxidative cleaning protocol (Barker et al., 2003; Rosenthal et al., 1997) and analyzed at Rutgers Inorganic Analytical Laboratory using a Sector Field Inductively Coupled Plasma Mass Spectrometer (Thermo Element XR) following the methods outlined in Rosenthal et al. (1999). The long-term analytical precision of Mg/Ca ratios is based on three consistency standards of Mg/Ca concentrations of 1.10, 2.40 and 6.10 mmol mol$^{-1}$. Over the course of this study, the precision for the consistency standards was 1.6, 1.2 and 1.2% RSD (relative standard deviation) respectively. For paleotemperature reconstructions the equation Mg/Ca = 0.49 T (°C) was used (Rosenthal et al., 2011). Standard-error estimates for paleotemperature, the oxygen isotopic composition of seawater ($\delta^{18}O_{sw}$), salinity and density values are ±0.7 °C, ±0.3‰, ±0.7 psu and $\sigma_\ominus = \pm 0.3$, respectively. However, modern calculated salinities and densities fall within ±0.30 psu and $\sigma_\ominus = \pm 0.2$ based on modern paired Mg/Ca–$\delta^{18}O_{sw}$ measurements of *H. Balthica* from Cape Ghir (Rosenthal et al., 2011). To calculate error margins on temperature, $\delta^{18}O_{sw}$, and salinity, we followed standard error propagation calculations for a quadratic paleotemperature equation (Shackleton, 1974), including measurement and calibration errors, uncertainties in the freshwater end-member of the modern $\delta^{18}O_{sw}$–salinity relationship, and uncertainties in estimates for global ice-volume changes (Schmidt, 1999). We assumed a constant $\delta^{18}O_{sw}$–salinity relationship for down-core salinity reconstructions. Finally, $\delta^{18}O$ and $\delta^{13}C$ core-top records were not found to be significantly correlated at the $\alpha = 0.05$ significance level ($r = 0.11$, $n = 27$, $p = 0.95$, *t-test* = 0.069, *critical t* = 2.06). For all regression analyses, time series were linearly interpolated using the lower resolution of the two series as common resolution. The significance of all correlations used in this study is tested by determining the *t-score* on the slope of the regression between two parameters at the 95% confidence interval. If the *t-score* between two parameters is larger than the critical t value, the slope of the regression is statistically different to zero and the correlation between the arrays is significant.

## 3. Chronology

The age model for the top 78 cm of gravity core GeoB6007-2 was established based on a combination of published (Kuhlmann et al., 2004) and two additional accelerator mass spectrometry (AMS) radiocarbon measurements ($^{14}C$) (NOSAMS, Wood Hole Oceanographic Institution, see Table 1) at 56 and 70 cm, yielding $^{14}C$ ages of 1470 ± 60 and 1680 ± 85, respectively. All calibrated age errors are reported at the 2σ range. Mixed planktic species for AMS radiocarbon measurements included the following planktonic foraminifera: *Globigerina bulloides*, *Globigerina sacculifer*, *Globigerina calida*, *Globigerina ruber*, *Globigerina falconensis*, *Globigerina rubescens*, *Turborotalia quinqueloba*, and *Orbulina universa* (Kim et al., 2007; Kuhlmann et al., 2004). For a detailed description of the complete age model for sediment core GeoB6007-2 see Bamberg et al. (2010). To constrain the age of multicore GeoB6007-1, we measured an additional AMS radiocarbon date at 23 cm (460 ± 35 $^{14}C$ yrs) and stable carbon isotopes ($\delta^{13}C$) on the planktonic foraminifera *G. bulloides*. Measured $\delta^{13}C$ values for *G. bulloides*, range between ~−1.0‰ at the base and ~−1.8‰ at the top of the multicore (Fig. 3). All original AMS radiocarbon dates included in this analysis were recalibrated with Calib 5.0.2 and the atmospheric InCal04 calibration dataset (Stuiver et al., 1998; Stuiver and Reimer, 1993). We applied a reservoir age correction of 400 yrs for all dates and ages between calibrated dates were obtained by linear interpolation.

The calibrated AMS $^{14}C$ date of AD 1842 ± 40 (2σ) constrains the base of GeoB6007-1. The $\delta^{13}C$ record of the planktonic foraminifer *G. bulloides* supports this age determination by providing evidence for

**Table 1**
AMS $^{14}C$ radiocarbon dates for multicore GeoB6007-1 and gravity core GeoB6007-2.

| Lab ID* | Core | Depth (cm) | Species (planktic) | Radiocarbon Age ± 1σ error (yr BP) | Calibrated Age WMA (cal. kyr BP) | 2σ range (cal. kyr BP) | Calibrated Age WMA (cal. yr AD) | 2σ range (cal. yr AD) | Reference for original radiocarbon dates |
|---|---|---|---|---|---|---|---|---|---|
| OS-73652 | GeoB6007-1 | 4 | *Mixed species* | >Mod | x | x | x | x | This study |
| OS-72997 | GeoB6007-1 | 23 | *Mixed species* | 460 ± 35 | 0.106 | 0.067–0.142 | 1842 | 1808–1883 | This study |
| KIA 20537 | GeoB6007-2 | 3 | *Mixed species* | 285 ± 35 | Modern | Modern | Modern | Modern | Kuhlmann et al., 2004 |
| OS-73175 | GeoB6007-2 | 56 | *Mixed species* | 1470 ± 60 | 0.975 | 0.889–1.024 | 973 | 926–1061 | This study |
| OS-73654 | GeoB6007-2 | 70 | *Mixed species* | 1630 ± 85 | 1.129 | 0.944–1.316 | 818 | 634–1006 | This study |
| KIA 20536 | GeoB6007-2 | 78 | *Mixed species* | 1695 ± 35 | 1.206 | 1.113–1.295 | 742 | 655–818 | Kuhlmann et al., 2004 |
| KIA 16976 | GeoB6007-2 | 148 | *G. bulloides* | 2840 ± 30 | 2.546 | 2.465–2.638 | 598 BC | 689–516 BC | Kuhlmann et al., 2004 |

* (KIA) Leibniz-Laboratory for Radiometric Dating and Stable Isotope Research (OS) The National Ocean Sciences Accelerator. Mass Spectrometry Facility (NOSAMS).

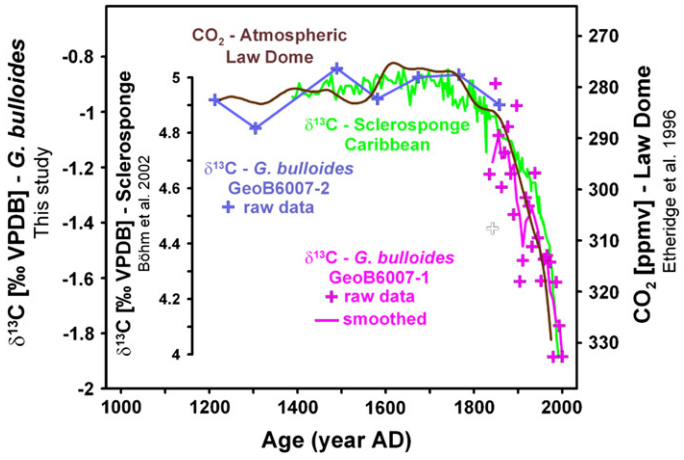


**Fig. 3.** Suess effect: The comparison of the Caribbean sclerosponge $\delta^{13}C$ (‰ VPDB) record (Böhm et al., 2002) with atmospheric $CO_2$ reconstructions from the Law Dome Ice core record (Etheridge et al., 1996) and the $\delta^{13}C$ (‰ VPDB) from GeoB6007-1 (magenta) and GeoB6007-2 (dark blue) illustrate the rapid depletion of oceanic $\delta^{13}C$ values in conjunction with rising atmospheric $CO_2$ values over the past 165 yrs.

the imprint of the anthropogenic $CO_2$ increase on the marine carbon isotope composition throughout the length of the multicore, exemplified by a sharp decrease in $\delta^{13}C$ values. This decrease reveals the presence of the '$\delta^{13}C$ Suess effect', indicating the oceanic uptake of isotopically light $CO_2$ released by the burning of fossil fuel since the early 19th century (Keeling et al., 1979). Available reconstructions for total sea surface $\delta^{13}C$ depletion based on corals and sclerosponges from the Caribbean and Florida range between 0.7 and 0.9‰ since the early 19th century (Böhm et al., 2002; Swart et al., 2010). This estimate is consistent with the total decrease of ~0.7‰ observed in the $\delta^{13}C$ record of *G. bulloides* in GeoB6007-1 (Fig. 3). Considering that the total range of the anthropogenic Suess effect appears to be present in GeoB6007-1 and pre-industrial values are also present in the oldest part of the multicore, the base of GeoB6007-1 cannot be much younger than 1850 AD. This age constraint is consistent with $\delta^{13}C$ records from the subtropical North Atlantic (Böhm et al., 2002) and atmospheric $CO_2$ reconstructions from Law Dome, Antarctica (Etheridge et al., 1996); which provide evidence for a significant decrease in $\delta^{13}C$ in the ocean and increased atmospheric $CO_2$ by 1850 compared to pre-industrial values. The absence of a plateau in the $\delta^{13}C$ record at pre-industrial values (Fig. 3) further constrains the oldest possible date for the core to the early 19th century, before which oceanic $\delta^{13}C$ and atmospheric $CO_2$ values did not significantly vary beyond Late Holocene variability (Böhm et al., 2002; Etheridge et al., 1996). The agreement between the $\delta^{13}C$ age constraint (1800–1850 AD) at the base of the multicorer with the $^{14}C$ AMS date of 1842 AD ±40 yrs at 23 cm allows us to interpret the paleoceanographic record from GeoB6007-1 with confidence. The age model for GeoB6007-2 determines the start of the Late Holocene record to be at ~1184± 105 yrs BP (816 ± 105 yrs AD) (2σ) (Table 1).

## 4. Results

### 4.1. Geochemical and statistical analysis on GeoB6007-1

High resolution (1 cm) Mg/Ca measurements on GeoB6007-1 indicate that bottom water temperature (BWT) cooled by 0.7–1.0 °C since ~1842 AD to reach modern bottom water values of 7.6–7.8 °C (Fig. 4). These results from the core top sample are consistent with measured BWT at 900 m depth of 7.8–7.9 °C in 1993 and 1997 (Knoll et al., 2002). The good agreement between reconstructed and measured BWTs shows that Mg/Ca ratios from modern *H. balthica* tests reliably record in situ water temperatures at the core site.

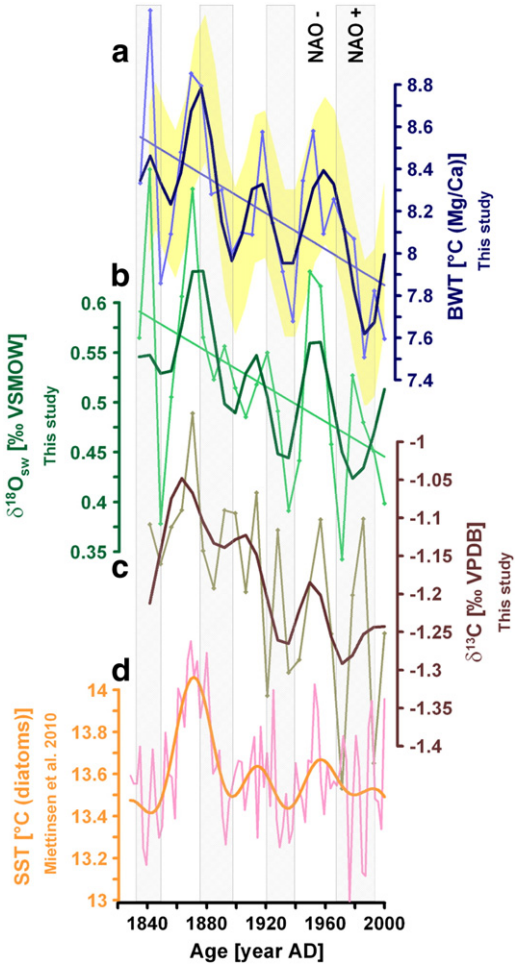


**Fig. 4.** Proxy records from GeoB-6007-1: (a) Mg/Ca based bottom water temperatures (BWT) and (b) $\delta^{18}O_{sw}$ estimates derived from paired Mg/Ca–$\delta^{18}O$ measurements. (c) show benthic (*H. balthica*) foraminiferal stable carbon isotopes ($\delta^{13}C$ ‰ vs. VPDB). Also shown is (d) a sea-surface temperature (SST) record from the subpolar gyre (Miettinen et al. 2010). All graphs are plotted versus age (for age model see Table 1 and Fig. 2) and 30 yr low-pass filters are shown in bold. Also shown are the error envelopes for the temperature reconstructions (for the 30 yr low pass filter).

On multidecadal timescales the cross-correlations between BWT, salinities and the NAO index (Jones et al., 1997) are highest when all records are filtered using a windowed Fourier transform approach with cut-off periods of 30 and 60 yrs. At these periods, we consistently note that shifts from relatively warm to colder bottom waters occurred shortly after NAO shifts from negative to positive phases (Fig. 5). The significant correlation between BWT and $\delta^{18}O_{sw}$ ($r=0.52$, $n=23$, $p<0.05$) over the past 165 yrs further shows that a bottom water cooling generally concurred with a freshening at 900 m depth (Fig. 5). The highest cross-correlations between the NAO index and $\delta^{18}O_{sw}$ occur when the NAO index leads $\delta^{18}O_{sw}$ by 1 cm ($r=0.65$, $n=22$, $p<0.05$) which would correspond to about a decade if the variations on surface reservoir ages associated with the dating uncertainties could be neglected. Similarly the correlation between NAO and BWT is also strongest when the NAO leads BWT by a decade. Only for the most recent samples (~1980's onward) the correlation between BWT and NAO appears to break down, resulting in a weaker and less significant overall correlation between the two parameters (Fig. 5). When the top 3 samples are removed the correlation is significant ($r=0.66$, $n=19$, $p<0.05$). BWT and $\delta^{13}C$ values do not cross-correlate at these frequencies, neither in phase nor at an offset to each other. However, $\delta^{13}C$ values and the NAO index cross-correlate significantly when in phase with each other ($r=0.41$, $n=23$, $p<0.05$).

Additionally we compare a high resolution subpolar SST record with our BWT and $\delta^{18}O_{sw}$ results as well as with the NAO index. This record based on fossil diatom assemblages and collected by Miettinen et al. (2010) from the eastern flank of the Gardar drift (56°N, 28°W) provides SST data from the formation region of SPMW over the past 230 yrs (Fig. 4). A strong correlation exists between the subpolar SST and the NAO record ($r=0.81$, $n=22$, $p<0.05$) when both records are in phase with each other at multidecadal timescales (Fig. 5). Similar to the correlation between BWT and the NAO index, the cross correlation between BWT and subpolar SST is most significant when SST and BWT are offset by about a decade ($r=0.56$, $n=22$, $p<0.05$).

Finally, we plot temperature and salinity results among equal density lines on a local temperature–salinity plot (Fig. 6). The results show that the lightest densities recorded over the past 165 yrs occurred in the late 1970's and early 1930's ($\sigma_\theta \approx 27.5$), two periods that correspond to NAO (+) years while heaviest densities occurred during the late 1950's and 1860's ($\sigma_\theta \approx 27.7$), which correspond to NAO (−) years (Fig. 6).

### 4.2. Geochemical and statistical analysis on GeoB6007-2

Mg/Ca measurements from gravity core GeoB6007-2 indicate a long-term, step-like cooling of 0.8–1.0 °C throughout the record (Fig. 7). Multidecadal intervals of colder BWT are centered between 1250–1350 AD, 1475–1550 AD and 1625–1725 AD and intervals of warmer BWT occurred between 850–900 AD, 1100–1200 AD and 1400–1450 AD. To test the multidecadal relationship among BWT, $\delta^{18}O_{sw}$ and ΔTSI (Steinhilber et al., 2009) over the past 1200 yrs, all records were bandpass-fitted using cut-off periods of 60 and 100 yrs (Fig. 8) in order to focus on the multidecadal solar Gleissberg cycle (70–90 yrs) (Reid, 1991). Similar to the multicore results, the $\delta^{18}O_{sw}$ and BWT records from GeoB6007-2 correlate well with each other ($r=0.56$, $p<0.05$, $n=98$) at these frequencies and are most significant ($r=0.69$, $p<0.05$, $n=97$) if $\delta^{18}O_{sw}$ leads BWT by about a decade. These results show that a cooling in BWT occurred in phase with or shortly after a freshening during the past 1200 yrs. The correlation between BWT and ΔTSI is also significant ($r=0.53$, $p<0.05$, $n=96$) when ΔTSI leads BWT by ~20 yrs (2 cm). This cross-correlation indicates that cool episodes recorded in the BWT record are correlated with solar minima. The correlation between ΔTSI and $\delta^{18}O_{sw}$ is most significant ($r=0.38$, $p<0.05$, $n=97$) when ΔTSI leads $\delta^{18}O_{sw}$ by ~10 yrs (1 cm), in agreement with the offset between BWT and $\delta^{18}O_{sw}$. We stress that the offset between BWT and $\delta^{18}O_{sw}$ is robust since both measurements were taken from the same sample. All other offsets remain within the uncertainties associated with our and the ΔTSI age model.

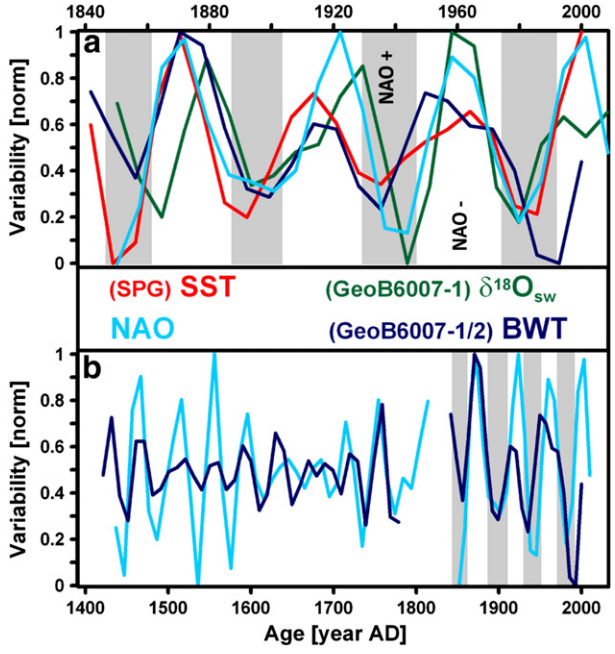


**Fig. 5.** Variability: a) Comparison of the multi-decadal bandpass filters (30 and 60 yr cut off periods) for the instrumental NAO index (Jones et al., 1997) subpolar gyre (SPG) sea surface temperatures (Miettinen et al., 2010) with the variability in bottom water temperatures and $\delta^{18}O_{sw}$ from GeoB6007-1. All records are normalized between 0 and 1. Both the NAO index and $\delta^{18}O_{sw}$ have been shifted by 1 cm to account for the identified offset. b) Comparison of the multi-decadal bandpass filters (30 and 60 yr cut off periods) for both the instrumental NAO index (Jones et al., 1997) and the reconstructed NAO index (Cook et al., 2002) (offset by ~30 yrs from the GeoB6007-2 age model) with reconstructed bottom water temperatures from both GeoB6007-1 and GeoB6007-2. Also shown are known intervals of positive (gray bars) and negative (white bars) phase shifts of the NAO index in panel a) and b).

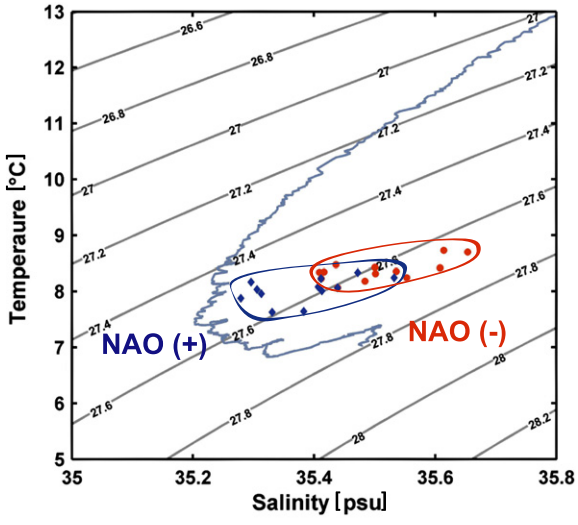


**Fig. 6.** GeoB6007-1 paleodensity reconstruction: Temperature and salinity results are plotted along density lines and compared to a local CTD cast (blue) (Knoll et al., 2002). Data points occurring in NAO (+) years are plotted in blue and data points falling into NAO (−) years are plotted in red. The results indicate that densities are generally lighter during NAO (+) years (blue circle) then during NAO (−) years (red circle) over the past 165 yrs.

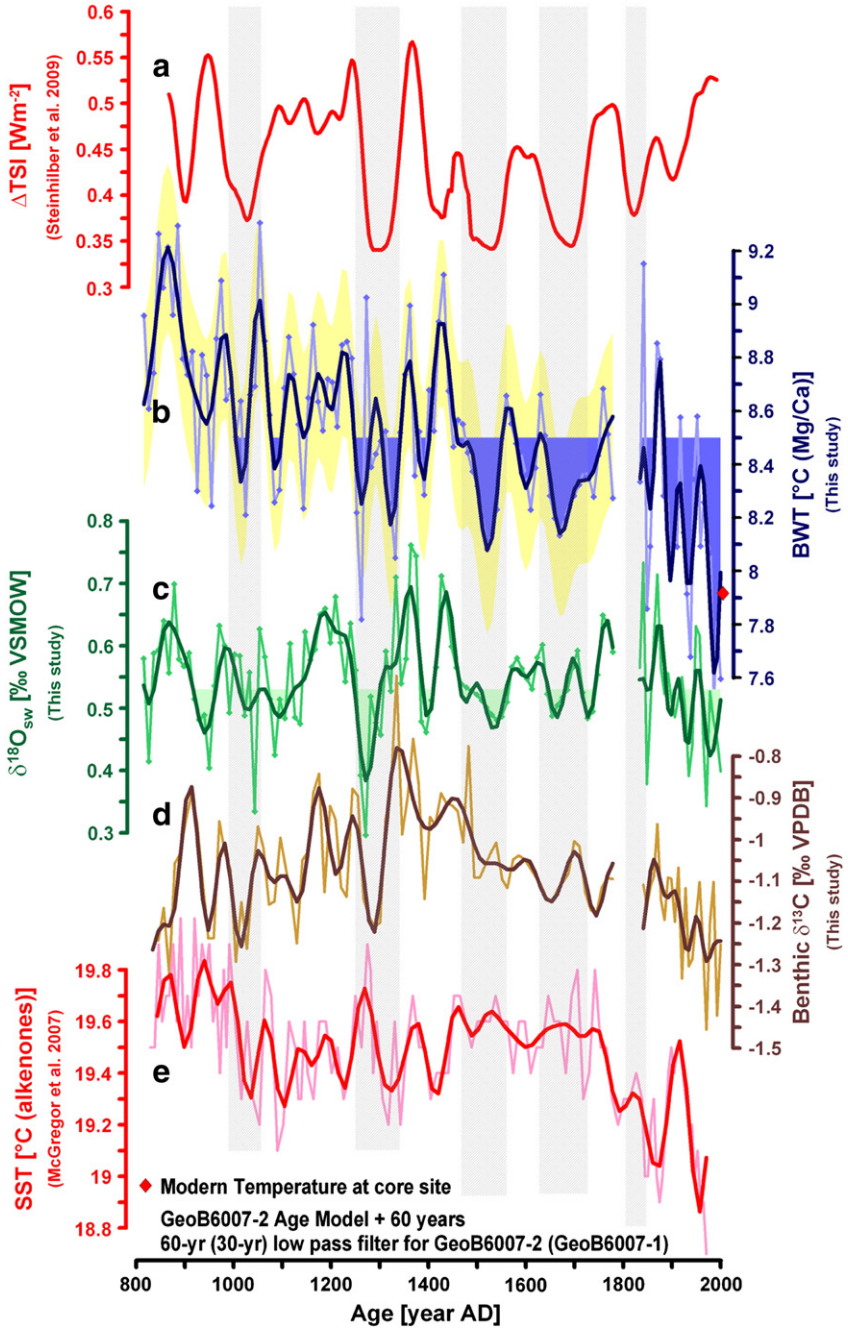


**Fig. 7.** Proxy records from GeoB-6007-2: Here we compare (a) reconstructed solar variability ΔTSI ($Wm^{-2}$) with (b) Mg/Ca based bottom water temperatures (BWT) and (c) $\delta^{18}O_{sw}$ estimates derived from paired Mg/Ca–$\delta^{18}O$ measurements. Also shown are (d) benthic (*H. balthica*) foraminiferal stable carbon isotopes ($\delta^{13}C$ ‰ VPDB) and (e) late Holocene sea surface temperature (SST) reconstructions off Northwest Africa based on the combined record of multicore GeoB6008-2 and gravity core GeoB6008-1. The SST record is normalized to the average for 1912–1971, the period when GeoB6008-2 and GeoB6008-1 overlap (McGregor et al., 2007). All graphs are plotted versus age (for age model see Table 1) and 60 yr low-pass filters are shown in bold. Also shown are the error envelopes for the temperature reconstructions (for the 60-yr filter). Gray bars indicate solar minima of the Little Ice Age.

The $\delta^{13}C$ record from GeoB6007-2 yields no significant correlation with the BWT record, neither in phase ($r=0.04$, $p=0.61$, $n=98$) or at an offset, and thus agrees with the results from the multicore record. Further, we cross-correlated a local alkenone-based SST record from Cape Ghir (McGregor et al., 2007) with the benthic $\delta^{13}C$ data and obtained a significant correlation ($r=0.65$, $p<0.05$, $n=96$) (Fig. 8). Finally, reconstructed density profiles at the core site (Fig. 9), show a tendency towards lighter density surfaces during minima of ΔTSI ($\sigma_\theta \approx 27.45$) compared to maxima in ΔTSI ($\sigma_\theta \approx 27.8$) (Fig. 9) throughout the Late Holocene.

## 5. Discussion

### 5.1. Multidecadal variability over the past 165 years

Two possible mechanisms may explain the relationship between reconstructed $\delta^{18}O_{sw}$, BWT, and the NAO at GeoB6007-1. First, the depth of the eastern STG thermocline may be related to the NAO. Enhanced northeast trade winds off the Northwest African coast during NAO (+) phases promote upward Ekman pumping and may result in a shoaling of the STG thermocline (Curry and McCartney,

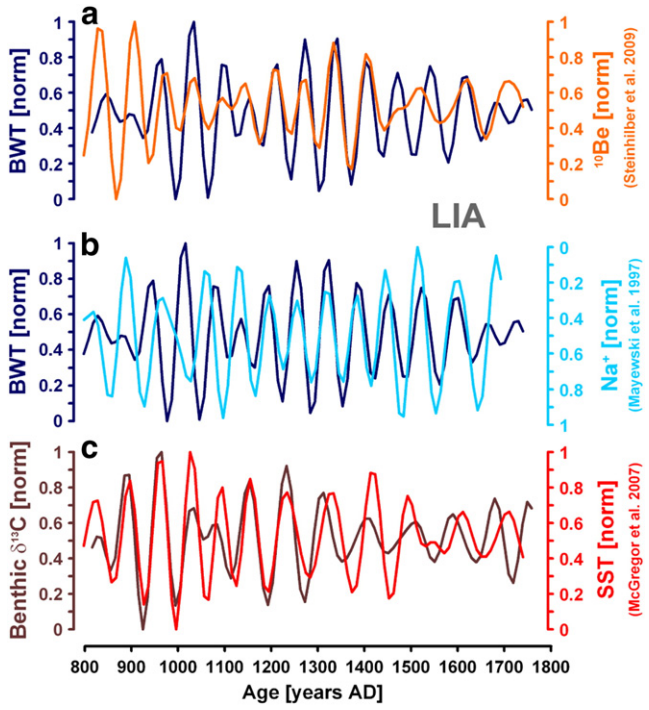


**Fig. 8.** Late Holocene Variability: Comparison of the multi-decadal to centennial band-pass filters (60 and 100 yr cut off periods) of (a) bottom water temperatures (BWT in dark blue) with solar variability (ΔTSI in orange) (b) bottom water temperatures (BWT in dark blue) with the sea salt sodium record ($Na^+$ in light blue) from GISP2, Central Greenland and (c)benthic stable carbon isotopes ($\delta^{13}C$ in brown) and sea surface temperatures (SST in red) (McGregor et al., 2007). All records are normalized between 0 and 1.

2001). A shoaling at 900 m depth may then allow the incursion of relatively cooler and fresher AAIW at the core site. Alternatively, the covariance between temperature, $\delta^{18}O_{sw}$, and NAO may originate from the north and correspond to the production of cooler and fresher SPMW during NAO (+) years that travel south within ENACW into the eastern boundary of the STG (Fig. 5) (Keffer, 1985; Levitus, 1989; McCartney and Talley, 1982; McDowell et al., 1982). Here we discuss these two alternatives by combining observations and results from instrumental and reconstructed proxy records from both gyres.

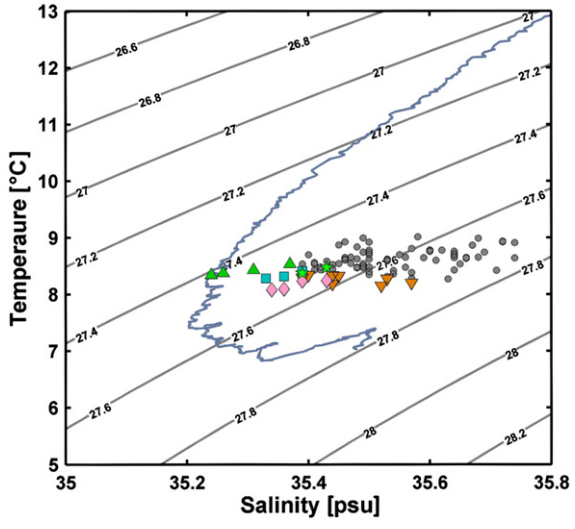


**Fig. 9.** GeoB6007-2 paleodensity reconstruction: Temperature and salinity results from AD 800 to 1800 are plotted along density lines and compared to a local CTD cast (blue) (Knoll et al., 2002). Data points occurring during the Little Ice Age solar minima are plotted in green triangles/stars (Wolf Minimum), blue rectangles (Oort Minimum), pink lozenges (Spörer Minimum) and inverted orange triangles (Maunder Minimum). The remaining data points are plotted in gray circles. The results show that densities are generally lighter during solar minima of the Late Holocene.

### 5.2. Thermocline shoaling in the Subtropical Gyre

Driven by the intensification of mid-latitude westerlies, STG water mass circulation is high during positive NAO years. Especially in the western boundary this intensification results in a significant shoaling of the thermocline (100–1200 m) (Curry and McCartney, 2001). This vertical displacement of the thermocline in response to changes in zonally integrated wind stress fields has also been successfully modeled (Sturges et al. 1998, Frankignoul et al. 1997) supporting that the thermocline depth in the western STG is primarily wind forced and linked to NAO phase shifts. However, evidence for a thermocline shoaling in the eastern boundary of the STG at 900 m depth in conjunction with enhanced coastal trade winds during positive NAO years is weak. Curry and McCartney (2001) observed a slight shoaling of the eastern STG thermocline in the upper 300 to 800 m during the 1990s relative to the 1965–1974 time interval (from NAO (−) towards NAO (+)). However, water masses below 800 m did not experience a vertical displacement due to local Ekman pumping. This agrees with earlier observations by Levitus (1989) showing that eastern STG shoaling during NAO (+) phases only occurred on density surfaces between $\sigma_\theta \approx 26.5$ and 27.3 whereas no significant upward displacement had been recorded below 800 m or $\sigma_\theta > 27.3$. Additionally, several studies indicate that the production and northward extent of AAIW weakened over the past 50 yrs (Curry et al., 2003; Goes et al., 2008), suggesting weaker rather than increased influence of this colder and fresher water-mass at the core site.

The insignificant correlation between the benthic $\delta^{13}C$ and BWT time series throughout GeoB6007-1 suggests that STG thermocline depth variations are not the predominant forcing for temperature and salinity changes at the core site. Similar to other shallow infaunal foraminifera species, *H. balthica* records change in local oceanic productivity/upwelling in the $\delta^{13}C$ values measured from their shell lattice (Bamberg et al., 2010; McCorkle et al., 1990; Schmiedl et al., 2004; Tachikawa and Elderfield, 2002). An increase in local upwelling off Cape Ghir in conjunction with NAO (+) years will likely enhance sea surface productivity and intensify the availability and decomposition of organic matter at 900 m depth. As a result, steeper dissolved organic carbon gradients are expected to develop within the top centimeters of surface sediments that should result in more depleted $\delta^{13}C$ values recorded in *H. balthica* tests during times of increased upwelling.

The correlation between $\delta^{13}C$ and the NAO index over the past 165 yrs suggests that NAO modulated local trade winds enhanced productivity off the Northwest African coast at multidecadal timescales. However, the insignificant correlation between the BWT and the $\delta^{13}C$ records suggests that NAO-forced upwelling at the sea surface did not result in a shoaling of the thermocline and an incursion of cooler AAIW at the core site.

There is however, no clear correlation between the local alkenone-based SST reconstructions and the NAO index on decadal timescales (McGregor et al., 2007). Instead McGregor et al. (2007) related the recent SST cooling observed over the past 50 yrs to $CO_2$ forced global warming ("Bakun hypothesis"), whereby the global temperature increase enhances the sea surface–land surface temperature gradients, which in turn force enhanced coastal wind intensity and thus upwelling (Bakun, 1990; Narayan et al., 2010). This anthropogenic forcing may have overprinted NAO-modulated SST cooling and may thus explain the lack in correlation between reconstructed SST and NAO at GeoB6008-2. Nevertheless, we suggest that the consistent

offset between BWT, $\delta^{13}C$ and NAO indicates that the NAO signal recorded in BWT reaches the core site with about a decade delay and, most importantly, that NAO induced upwelling and Ekman pumping at Cape Ghir does not result in a shoaling of the base of the eastern STG thermocline nor in an incursion of AAIW at the core site.

### 5.3. North Atlantic Central Water circulation and climate signal propagation

Iselin (1936) originally suggested southward flow and the ventilation of the eastern boundary of the STG by SPMW. In the early 1980's McCartney and Talley (1982) drew the first mid-depth potential vorticity maps, providing physical evidence for southward flow along density surfaces $\sigma_\ominus = 27.3$ to 27.6 from the SPG into the STG. Moreover, McDowell et al. (1982), Keffer (1985) and Levitus (1989) later confirmed, based on additional observations, that the potential vorticity distribution for this surface allows water parcels to move southward underneath the North Atlantic Current from the region just south of Iceland into the STG to ~30°N before turning southwestward into the southern STG (Fig. 2).

Assuming that these processes occurring over the past 50 yrs have operated during the past millennium, we would expect to observe the following: (a) a significant correlation between subpolar SST and the NAO index over the past 165 yrs (within the age uncertainty of their age models) and (b) the strongest correlation between subtropical BWT and subpolar SSTs should exist at a lag similar to our observed offset between BWT and NAO to account for signal transfer into subtropical latitudes. The consistent offset between BWT and the NAO, subpolar SST, and subtropical $\delta^{13}C$ values strongly supports our interpretation whereby the southward flow of ENACW and ventilation of the STG are NAO-modulated via SPMW formation.

The question remains whether NAO-induced surface water cooling and freshening of SPMW also weakens the production of ENACW, and whether the signal of this weakening is transferred to subtropical latitudes via North Atlantic central water circulation. Paleodensity estimates (Fig. 6) indicate that even though some of the changes between NAO (+) and NAO (−) years are density-compensated (occur along a single density surface), the lightest densities recorded over the past 165 yrs occurred during two periods that correspond to NAO (+) years whereas heaviest densities occurred during periods which correspond to NAO (−) years (Fig. 6). These results suggest that similar to North Atlantic Deep Water production in the Nordic Seas and Iceland Scotland Overflow Water strength (Boessenkool et al., 2007; Eden and Jung, 2001), ENACW formation south of Iceland weakens during NAO (+) phase shifts.

### 5.4. Atmosphere–ocean solar signal transfer from the SPG into the mid-depth STG

The significant correlation between the benthic $\delta^{13}C$ (*H.balthica*) and local SST variability (McGregor et al., 2007) at multidecadal timescales suggests that similar to the past 165 yrs, sea-surface processes off Cape Ghir were locally controlled by the easterly trade winds during the past 1200 yrs. The clear decoupling of $\delta^{13}C$ and overlying SST signals from BWT and ΔTSI (Fig. 8) further supports that BWT at 900 m depth are modulated by SPG atmosphere–ocean processes and not by an incursion of AAIW. The decoupling between surface and central water processes becomes evident especially during the main phase of the Little Ice Age from 1300 to 1850 AD. During the Little Ice Age, the variability in ENACW temperatures significantly correlates with the reconstructed NAO index (Cook et al., 2002) ($r = 0.64$, $n = 35$, $p < 0.05$), linking cold ENACW with NAO (+) phase shifts, similar to the results observed over the past 165 yrs (Fig. 5). The Cook et al. (2002) NAO index combines numerous records from the eastern, western, and polar North Atlantic realm and thus provides a comprehensive signature of past NAO cycles on the North Atlantic region. The correlation of past ENACW temperatures with a European based NAO reconstruction (Trouet et al., 2009) is significant ($r = 0.35$, $n = 75$, $p < 0.05$), but weaker.

On longer timescales, assuming that similar to recent multidecadal processes, the recorded BWT at the core site reflects subpolar atmosphere–ocean processes, the significant correlation between colder BWT and ΔTSI minima (Fig. 8) suggests that subpolar surface waters were colder and fresher during solar minima. In line with this interpretation, a suite of established proxy records covering polar-, subpolar- and the mid-latitudes of the Northeast Atlantic realm provides evidence for enhanced atmospheric circulation during solar minima of the LIA (Jackson et al., 2005; Keigwin, 1996; Kreutz et al., 1997; Meeker and Mayewski, 2002). At polar latitudes the high resolution sodium ($Na^+$) record from GISP2 in central Greenland, a proxy for the strength of the Icelandic Low (Mayewski et al. 1997, Meeker and Mayewski, 2002), displays sharp increases in $Na^+$ and thus intensifications of the Icelandic Low during solar minima of the LIA. Compared to ENACW temperatures from GeoB6007-2 (Fig. 8) we note a strong correlation ($r = -0.53$, $n = 90$, $p < 0.05$) between the strength of the Icelandic Low and the formation of colder ENACW at multidecadal timescales (60–100 yr) especially from AD 1100 to 1800. Additional evidence for enhanced winter storminess during the LIA, has also been recorded in western Norway where the growth of maritime glaciers indicates enhanced winter precipitation (~25%) in combination with lowered winter temperatures (~0.5 °C) during the LIA (Nesje et al., 2008; Rasmussen et al., 2010). Numerous coastal storm deposits in Ireland (Wilson et al., 2004; Wintle et al., 1998), Scotland (Outer Hebrides) (Dawson et al., 2004; Gilbertson et al., 1999), and Sweden (Jong et al., 2006) as well as loess deposits from southern Iceland (Jackson et al., 2005) dating to the LIA provide further evidence for intense storms passing over Northern Europe during this period. Evidence for colder sea surface temperatures in the northeastern SPG during solar minima of the LIA is also given by a suite of subpolar SST and drift ice studies, that support a positive relationship between solar forcing and subpolar SST's (Jiang et al., 2005; Lohmann et al., 2004; Moros et al., 2006; Ran et al., 2010; Sicre et al., 2008) similar to observations made during recent NAO (+) phase shifts (Nesje et al., 2008). The tendency towards lighter density surfaces during solar minima ($\sigma_\theta \approx 27.45$) compared to solar maxima ($\sigma_\theta \approx 27.8$) (Fig. 9) additionally supports cooler and lighter sea surface conditions during the LIA.

The discussed high latitude atmospheric (Greenland) and sea surface temperature records from the northeastern SPG as well as coastal records from Northern Europe are apparently at odds with a NAO (−) like structure that has been put forward by several GCM studies (Mann et al., 2009; Shindell et al., 2001a) and some (but not all see Cook et al., 2002) reconstructions of the NAO index during the LIA (Trouet et al., 2009) and thus stand in sharp contrast with the assumption that the westerly airflow was reduced during the LIA especially over the subpolar North Atlantic and Northern Europe (Mann et al., 2009; Richter et al., 2009; Shindell et al., 2001a; Trouet et al., 2009). In support of the link between solar minima and NAO (−) phase shifts, Thornalley et al. (2009) record a thermocline warming in the northeastern SPG between 1300 and 1800 AD. In line with SPG dynamics during NAO (−) phase shifts Thornalley et al. (2009) associate the subsurface warming with a northwestern retreat of the gyre and an increased influence of warm Atlantic waters into the southeastern SPG during the coldest interval of the LIA. A distinct sea surface warming recorded in Feni Drift between AD 1600 and 1800 supports Thornalley's interpretation (Richter et al. 2009). However, several sea surface investigations from the Gulf of Mexico and Caribbean Sea (Goodkin et al., 2008; Haase-Schramm et al., 2003; Richey et al., 2009), provide evidence for cooler Atlantic waters at the source of the North Atlantic Current (NAC). Colder SST's in the Gulf of Mexico and Caribbean Sea are not only consistent with an increase in the north–south sea-level pressure gradient and NAO (+) phase shifts,

but would also result in colder Atlantic waters within the NAC. Although these records are seemingly at odds with the results provided by Thornalley et al. (2009) and Richter et al. (2009) we would like to note that NAO induced changes in the subtropics may be overprinted further downstream by dynamical changes in the SPG, affecting the freshwater budget of SPG surface waters.

A possible explanation for the apparent discrepancy in the data may be provided by simulations of the cyclone-resolving Climate Community System Model (CCSM) coupled ocean–atmosphere general circulation model for the Maunder Minimum (LIA) (Raible et al., 2007). These authors propose that major mid-latitude blocking anticyclones reduce cyclone frequency during the LIA consistent with NAO (−) phases. However the intensity of cyclones is increased when anticyclones break down. The enhanced storminess recorded by the ice core, sea surface, and coastal proxies may therefore be a result of more intense, rather than more frequent, winter storms during the LIA (Raible et al., 2007; Scourse et al., 2010).

Additionally, seasonal changes should be considered., *G. bulloides and* the thermocline dweller *Globorotalia inflata* used to reconstruct surface and thermocline temperatures in the northeastern SPG (Richter et al., 2009; Thornalley et al., 2009) are early to mid-summer bloomers, with largest abundances from June to August and lowest during the winter months (Dez-Mar) (Chapman, 2010). The downcore temperature records based on these species are thus most likely biased towards summer temperatures. Luterbacher et al. (2004) proposed that most of the cooling associated with the LIA occurred during winter and spring while summer temperatures did not depart from the 20th century average. Accordingly, the relative thermocline warming recorded in the northeastern SPG may represent a seasonal response pattern of the SPG, or in the time of foraminiferal blooms during the LIA. The regionally and possibly seasonally different response patterns of sea surface, subsurface, coastal and atmospheric records to Late Holocene climate forcing illustrate that the climate signatures associated with solar variability during the LIA are more complex than often assumed in the literature and that it may not be possible to generally associate them with either NAO state.

### 5.5. Central Water cooling over the past 165 yrs

Unlike the pre-industrial BWT–ΔTSI relationship, the ~0.8 °C BWT cooling trend over the past 165 yrs occurs during a period of increasing solar irradiance. This cooling trend (<0.8 °C) suggests that sea surface heat loss due to stronger westerly winds continually increased in the northeastern SPG since the early 19th century. This recent cooling trend is also present in SST proxy reconstructions (Hall et al., 2010; Richter et al., 2009) and in instrumental SST datasets from the northeastern SPG (Xue et al., 2003) all supporting the cross gyre climate signal transfer mechanism suggested in this study. An apparent eastward shift of the center of NAO activity from the southwestern tip of Greenland towards Iceland (Furevik and Nilsen, 2005) may explain the NAO-modulated cooling trend observed in our record. This eastward shift significantly increased wind stress south of Iceland and may thus explain the colder BWT recorded in the STG. The reason for this shift is under debate.

## 6. Conclusions

The presented data indicate an intricate connection between the subpolar and subtropical gyres at mid-depth during the past 165 yrs and throughout the late Holocene. Further, we conclude that central water temperatures and $\delta^{18}O_{sw}$ values recorded at 900 m depth in the eastern subtropical gyre are largely determined by Subpolar Mode Water formation south of Iceland and not by a thermocline shoaling and an incursion of fresher and cooler Antarctic Intermediate Water. The sensitive response of Subpolar Mode Water formation to changes in atmosphere-ocean processes permits the transfer of climate variability to Eastern North Atlantic Central Waters (Johnson and Gruber, 2007) and thereby links central water circulation with the NAO and solar variability on multidecadal to centennial timescales. These findings stress the importance of atmosphere–ocean linkages in the northeastern subpolar gyre for the spatial and temporal nature of climate signal propagation within the central eastern North Atlantic and underline the importance of cross-gyre central water transport underneath the North Atlantic Current for understanding the full range of meridional heat transfer between the subpolar and subtropical North Atlantic. The strong evidence for either NAO (−) or NAO (+) 'like' conditions during the LIA raises important questions about the suitability of characterizing past ocean–atmosphere linkages with modern indices and the need to consider seasonal changes in future Late Holocene investigations.

The possible link between enhanced positive NAO phase shifts and increased greenhouse gas emissions (Furevik and Nilsen, 2005; Shindell et al., 2001a, 2001b), may lead to continued cooling of the eastern subtropical thermocline in the future. Regional numerical model analysis may help to constrain the underlying dynamics involved in cross-gyre climate signal transfer at central water depth and may also help to estimate the regional climate impact of stronger NAO (+) years and a continued thermocline cooling of the eastern subtrocpical thermocline.

## Acknowledgments

We thank M. Segl for stable isotope analyses and at the University of Bremen. We would also like to thank T. Babila and the trace metal geochemistry lab crew at IMCS, Rutgers University as well as Helge Meggers, Nikesh Narayan at the University of Bremen for advice and analytical support, the editor and an anonymous reviewer for thoughtful discussions and comments. The research was funded by the Deutsche Forschungsgemeinschaft INTERDYNAMIC DFG-Schwerpunktprogramm 1266 to AB, AP, SM, CR and MS.

## References

Ammann, C.M., Joos, F., Schimel, D.S., Otto-Bliesner, B.L., Tomas, R.A., 2007. Solar influence on climate during the past millennium: results from transient simulations with the NCAR Climate System Model. Proc. Natl Acad. Sci. 104, 3713–3718.
Arhan, M., Colin de Verdière, A., Mémery, L., 1994. The eastern boundary of the subtropical North Atlantic. Journal of Physical Oceanography 24, 1295–1316.
Bakun, A., 1990. Global climate change and intensification of coastal ocean upwelling. Sci. 247, 198–201.
Bamberg, A., Rosenthal, Y., Paul, A., Heslop, D., Mulitza, S., Rühlemann, C., Schulz, M., 2010. Reduced North Atlantic Central Water formation in response to early Holocene ice-sheet melting. Geophys. Res. Lett. 37, L17705.
Barker, S., Greaves, M., Elderfield, H., 2003. A study of cleaning procedures used for foraminiferal Mg/Ca paleothermometry. Geochemistry Geophysics Geosystems 4.
Böhm, F., Haase-Schramm, A., Eisenhauer, A., Dullo, W.C., Joachimski, M.M., Lehnert, H., Reitner, J., 2002. Evidence for preindustrial variations in the marine surface water carbonate system from coralline sponges. Geochem. Geophys. Geosyst. 3, 1019.
Chapman, M.R., 2010. Seasonal production patterns of planktonic foraminifera in the NE Atlantic Ocean: Implications for paleotemperature and hydrographic reconstructions. Paleoceanography 25, PA1101.
Cook, E.R., D'Arrigo, R.D., Mann, M.E., 2002. A well-verified, multiproxy reconstruction of the winter North Atlantic Oscillation Index since a.d. 1400*. J. Climate 15, 1754–1764.
Curry, R.G., McCartney, M.S., 2001. Ocean gyre circulation changes associated with the North Atlantic Oscillation. J. Phys. Oceanogr. 31, 3374–3400.
Curry, R., Dickson, B., Yashayaev, I., 2003. A change in the freshwater balance of the Atlantic Ocean over the past four decades. Nature 426, 826–829.
Curry, R., Mauritzen, C., 2005. Dilution of the Northern North Atlantic Ocean in Recent Decades. Science 308, 1772–1774.
Dawson, S., Smith, D.E., Jordan, J., Dawson, A.G., 2004. Late Holocene coastal sand movements in the Outer Hebrides, N.W. Scotland. Mar. Geol. 210, 281.
Dickson, R.R., Osborn, T.J., Hurrell, J.W., Meincke, J., Blindheim, J., Adlandsvik, B., Vinje, T., Alekseev, G., Maslowski, W., 2000. The Arctic Ocean Response to the North Atlantic Oscillation. Journal of Climate 13, 2671–2696.
Dickson, B., Yashayaev, I., Meincke, J., Turrell, B., Dye, S., Holfort, J., 2002. Rapid freshening of the deep North Atlantic Ocean over the past four decades. Nature 416, 832–837.
Eberwein, A., Mackensen, A., 2006. Regional primary productivity differences off Morocco (NW-Africa) recorded by modern benthic foraminifera and their stable

carbon isotopic composition. Deep Sea Research Part I: Oceanographic Research Papers 53, 1379–1405.
Eberwein, A., Mackensen, A., 2008. Last Glacial Maximum paleoproductivity and water masses off NW-Africa: evidence from benthic foraminifera and stable isotopes. Marine Micropaleontology 67, 87–103.
Eden, C., Jung, T., 2001. North Atlantic Interdecadal Variability: Oceanic Response to the North Atlantic Oscillation (1865–1997). Journal of Climate 14, 676–691.
Etheridge, D.M., Steele, L.P., Langenfelds, R.L., Francey, R.J., Barnola, J.M., Morgan, V.I., 1996. Natural and anthropogenic changes in atmospheric $CO_2$ over the last 1000 years from air in Antarctic ice and firn. J. Geophys. Res. 101, 4115–4128.
Frankignoul, C., Müller, P., Zorita, E., 1997. A simple model of the decadal response of the ocean to stochastic wind forcing. Journal of Physical Oceanography 27, 1533–1546.
Furevik, T., Nilsen, J.E., 2005. Large-scale circulation variability and its impacts on the Nordic Seas Ocean climate — a review. In: Drange, H., Dokken, T., Furevik, T., Gerdes, R., Berger, W. (Eds.), The Nordic seas: an integrated perspective oceanography, climatology, biogeochemistry and modelling. the American Geophysical Union, Washington D.C, pp. 105–136.
Gilbertson, D.D., Schwenninger, J.L., Kemp, R.A., Rhodes, E.J., 1999. Sand-drift and soil formation along an exposed North Atlantic Coastline: 14,000 years of diverse geomorphological, climatic and human impacts. J. Archaeol. Sci. 26, 439.
Goes, M., Wainer, I., Gent, P.R., Bryan, F.O., 2008. Changes in subduction in the South Atlantic Ocean during the 21st century in the CCSM3. Geophysical Research Letters 35, L06701.
Goodkin, N.F., Hughen, K.A., Curry, W.B., Doney, S.C., Ostermann, D.R., 2008. Sea surface temperature and salinity variability at Bermuda during the end of the Little Ice Age. Paleoceanography 23, PA3203.
Haase-Schramm, A., Böhm, F., Eisenhauer, A., Dullo, W.-C., Joachimski, M.M., Hansen, B., Reitner, J., 2003. Sr/Ca ratios and oxygen isotopes from sclerosponges: temperature history of the Caribbean mixed layer and thermocline during the Little Ice Age. Paleoceanography 18, 1073.
Hall, I.R., Boessenkool, K.P., Barker, S., McCave, I.N., Elderfield, H., 2010. Surface and deep ocean coupling in the subpolar North Atlantic during the last 230 years. Paleoceanography 25, PA2101.
Hatun, H., Sando, A.B., Drange, H., Hansen, B., Valdimarsson, H., 2005. Influence of the Atlantic Subpolar Gyre on the thermohaline circulation. Sci. 309, 1841–1844.
Hebbeln, D., Meggers, H., N. S., Z. W., 1999. Report and preliminary results of METEOR Cruise M45/5a, North Atlantic 1999. In: Schott, F., Meincke, J., Meinecke, G. (Eds.), North Atlantic 1999, Cruise No. 45, 18 May–4 November 1999. METEOR-Berichte, Universität Hamburg, Hamburg, p. 161.
Hurrell, J.W., 1995. Decadal tends in the North Atlantic Oscillation: regional temperatures and precipitation. Sci. 269, 676–679.
Iselin, C.O.D., 1936. A study of the circulation of the western North Atlantic. Pap. Phys. Oceanorg. Meteorol. 4, 101.
Jackson, M.G., Oskarsson, N., TrÃ¡nes, R.G., McManus, J.F., Oppo, D.W., GrÃ¶nvold, K., Hart, S.R., Sachs, J.P., 2005. Holocene loess deposition in Iceland: Evidence for millennial-scale atmosphere–ocean coupling in the North Atlantic. Geol. 33, 509–512.
Jiang, H., Eiriksson, J., Schulz, M., Knudsen, K.-L., Seidenkrantz, M.-S., 2005. Evidence for solar forcing of sea-surface temperature on the North Icelandic Shelf during the late Holocene. Geol. 33, 73–76.
Johnson, G.C., Gruber, N., 2007. Decadal water mass variations along 20°W in the Northeastern Atlantic Ocean. Prog. Oceanogr. 73, 277–295.
Jones, P.D., Jonsson, T., Wheeler, D., 1997. Extension to the North Atlantic oscillation using early instrumental pressure observations from Gibraltar and south-west Iceland. Int. J. Climatol. 17, 1433–1450.
Jong, R.d., Björck, S., Björkman, L., Clemmensen, L.B., 2006. Storminess variation during the last 6500 years as reconstructed from an ombrotrophic peat bog in Halland, southwest Sweden. J. Quatern. Sci. 21, 905.
Katz, M.E., Cramer, B.S., Franzese, A., Honisch, B., Miller, K.G., Rosenthal, Y., Wright, J.D., 2010. Traditional and emerging geochemical proxies in foraminifera. J. Foramin. Res. 40, 165–192.
Keeling, C.D., Mook, W.G., Tans, P.P., 1979. Recent trends in the $^{13}C/^{12}C$ ratio of atmospheric carbon dioxide. Nat. 277, 121–123.
Keffer, T., 1985. The ventilation of the world's oceans: maps of the potential vorticity field. J. Phys. Oceanogr. 15, 509–523.
Keigwin, L.D., 1996. The Little Ice Age and Medieval Warm Period in the Sargasso Sea. Sci. 274, 1504–1508.
Kim, J.-H., Meggers, H., Rimbu, N., Lohmann, G., Freudenthal, T., Muller, P.J., Schneider, R.R., 2007. Impacts of the North Atlantic gyre circulation on Holocene climate off northwest Africa. Geol. 35, 387–390.
Knoll, M., Hernández-Guerra, A., Lenz, B., Laatzen, F.L., Machín, F., Müller, T.J., Siedler, G., 2002. The Eastern Boundary Current system between the Canary Islands and the African Coast. Deep-Sea Res. 49, 3427–3440.
Knudsen, M.F., Riisager, P., Jacobsen, B.H., Muscheler, R., Snowball, I., Seidenkrantz, M.-S., 2009. Taking the pulse of the Sun during the Holocene by joint analysis of $^{14}C$ and $^{10}Be$. Geophs. Research Lett. 36.
Kreutz, K.J., Mayewski, P.A., Meeker, L.D., Twickler, M.S., Whitlow, S.I., Pittalwala, I.I., 1997. Bipolar changes in atmospheric circulation during the Little Ice Age. Sci. 277, 1294–1296.
Kuhlmann, H., Meggers, H., Freudenthal, T., Wefer, G., 2004. The transition of the monsoonal and the N Atlantic climate system off NW Africa during the Holocene. Geophys. Res. Lett. 31, L22204.
Lean, J.L., 2010. Cycles and trends in solar irradiance and climate. Wiley Interdisciplinary Reviews. Climate Change 1, 111–122.
Levitus, S., 1989. Interpentadal variability of temperature and salinity at intermediate depths of the North Atlantic Ocean, 1970–1974 versus 1955–1959. J. Geophys. Res. 94, 6091–6131.
Lohmann, G., Rimbu, N., Dima, M., 2004. Climate signature of solar irradiance variations: analysis of long-term instrumental, historical, and proxy data. Int. J. Climatol. 24, 1045–1056.
Lockwood, M., Harrison, R.G., Woollings, T., Solanki, S.K., 2010. Are cold winters in Europe associated with low solar activity? Environmental Research Letters 5, 024001.
Luterbacher J. r., Dietrich, D., Xoplaki, E., Grosjean, M., Wanner, H., 2004. European seasonal and annual temperature variability, trends, and extremes since 1500. Sci. 303, 1499–1503.
Mann, M.E., Zhang, Z., Rutherford, S., Bradley, R.S., Hughes, M.K., Shindell, D., Ammann, C., Faluvegi, G., Ni, F., 2009. Global signatures and dynamical origins of the Little Ice Age and Medieval Climate Anomaly. Sci. 326, 1256–1260.
Mayewski, P.A., Meeker, L.D., Twickler, M.S., Whitlow, S.I., Yang, Q., Lyons, W.B., Prentice, M., 1997. Major features and forcing of high-latitude northern hemisphere atmospheric circulation using a 110,000-year-long glaciochemical series. J. Geophs Res. -Oceans 102 (C12), 26345–26366.
Marshall, J., Kushnir, Y., Battisti, D., Chang, P., Czaja, A., Dickson, R., Hurrell, J., McCartney, M., Saravanan, R., Visbeck, M., 2001a. North Atlantic climate variability: phenomena, impacts and mechanisms. International Journal of Climatology 21, 1863–1898.
Marshall, J., Johnson, H., Goodman, J., 2001b. A Study of the Interaction of the North Atlantic Oscillation with Ocean Circulation. Journal of Climate 14, 1399–1421.
McCartney, M.S., Talley, L.D., 1982. The Subpolar Mode Water of the North Atlantic Ocean. J. Phys. Oceanogr. 12, 1169–1188.
McCorkle, D.C., Keigwin, L.D., Corliss, B.H., Emerson, S.R., 1990. The influence of microhabitats on the carbon isotopic composition of deep-sea benthic foraminifera. Paleoceanography 5, 161–185.
McDowell, S., Rhines, P., Keffer, T., 1982. North Atlantic potential vorticity and its relation to the general circulation. J. Phys. Oceanogr. 12, 1417–1436.
McGregor, H.V., Dima, M., Fischer, H.W., Mulitza, S., 2007. Rapid 20th-Century increase in coastal upwelling off Northwest Africa. Sci. 315, 637–639.
Meeker, L.D., Mayewski, P.A., 2002. A 1400-year high-resolution record of atmospheric circulation over the North Atlantic and Asia. Holocene 12, 257–266.
Meggers, H., Freudenthal, T., Nave, S., Targarona, J., Abrantes, F., Helmke, P., 2002. Assessment of geochemical and micropaleontological sedimentary parameters as proxies of surface water properties in the Canary Islands region. Deep Sea Research Part II 49, 3631–3654.
Miettinen, A., Koç, N., Hall, I., Godtliebsen, F., Divine, D., 2010. North Atlantic sea surface temperatures and their relation to the North Atlantic Oscillation during the last 230 years. Climate Dynamics 36, 533–543.
Moros, M., Andrews, J.T., Eberl, D.D., Jansen, E., 2006. Holocene history of drift ice in the northern North Atlantic: evidence for different spatial and temporal modes. Paleoceanography 21, PA2017.
Narayan, N., Paul, A., Schulz, M., 2010. Trends in coastal upwelling intensity during the late 20th century. Ocean Sci. 6, 815–823.
Nesje, A., Dahl, S., Thun, T., Nordli, Ø., 2008. The 'Little Ice Age' glacial expansion in western Scandinavia: summer temperature or winter precipitation? Climate Dynamics 30, 789.
Pérez, F.F., Pollard, R.T., Read, J.F., Valencia, V., Cabanas, J.M., Rios, A.F., 2000. Climatological coupling of the thermohaline decadal changes in Central Water of the Eastern North Atlantic. Scientia Marina 64, 347–353.
Poole, R., Tomczak, M., 1999. Optimum multiparameter analysis of the water mass structure in the Atlantic Ocean thermocline. Deep Sea Research Part I: Oceanographic Research Papers 46, 1895–1921.
Raible, C., Yoshimori, M., Stocker, T., Casty, C., 2007. Extreme midlatitude cyclones and their implications for precipitation and wind speed extremes in simulations of the Maunder Minimum versus present day conditions. Climate Dyn. 28, 409.
Ran, L., Jiang, H., Knudsen, K.L., Eiríksson, J., 2010. Diatom-based reconstruction of palaeoceanographic changes on the North Icelandic shelf during the last millennium. Palaeogeogr. Palaeoclimatol. Palaeoecol. 302, 109.
Rasmussen, L.A., Andreassen, L.M., Baumann, S., Conway, H., 2010. 'Little Ice Age' precipitation in Jotunheimen, southern Norway. Holocene 20, 1039–1045.
Reid, G.C., 1991. Solar total irradiance variations and the global sea surface temperature record. J. Geophys. Res. 96, 2835–2844.
Richey, J.N., Poore, R.Z., Flower, B.P., Quinn, T.M., Hollander, D.J., 2009. Regionally coherent Little Ice Age cooling in the Atlantic Warm Pool. Geophys. Res. Lett. 36, L21703.
Richter, T.O., Peeters, F.J.C., van Weering, T.C.E., 2009. Late Holocene (0–2.4 ka BP) surface water temperature and salinity variability, Feni Drift, NE Atlantic Ocean. Quat. Sci. Rev. 28, 1941–1955.
Rosenthal, Y., Boyle, E.A., Slowey, N., 1997. Temperature control on the incorporation of magnesium, strontium, fluorine, and cadmium into benthic foraminiferal shells from Little Bahama Bank: Prospects for thermocline paleoceanography. Geochimica et Cosmochimica Acta 61, 3633–3643.
Rosenthal, Y., Field, M.P., Sherrell, R.M., 1999. Precise determination of element/calcium ratios in calcareous samples using sector field inductively coupled plasma mass spectrometry. Analytical Chemistry 71, 3248–3253.
Rosenthal, Y., Morley, A., Barras, C., Katz, M.E., Jorissen, F., Reichart, G.-J., Oppo, D.W., Linsley, B.K., 2011. Temperature calibration of Mg/Ca ratios in the intermediate water benthic foraminifer Hyalinea balthica. Geochem. Geophys. Geosyst. 12, Q04003.
Sarnthein, M., Thiede, J., Pflaumann, H., Erlenkeuser, H., Fütterer, D., Koopmann, D., Lange, H., Seibold, E., 1982. Atmospheric and oceanic circulation patterns off Northwest Africa during the past 25 million years. In: von Rad, H., Hinz, K., Sarnthein, M., Seibold, E. (Eds.), Geology of the Northwest African Continental Margin. Springer, Berlin, pp. 584–604.

Schmidt, G.A., 1999. Error analysis of paleosalinity calculations. Paleoceanography 14, 422–429.
Schmiedl, G., de Bovée, F., Buscail, R., Charrière, B., Hemleben, C., Medernach, L., Picon, P., 2000. Trophic control of benthic foraminiferal abundance and microhabitat in the bathyal Gulf of Lions, western Mediterranean Sea. Marine Micropaleontology 40, 167–188.
Schmiedl, G., Pfeilsticker, M., Hemleben, C., Mackensen, A., 2004. Environmental and biological effects on the stable isotope composition of recent deep-sea benthic foraminifera from the western Mediterranean Sea. Marine Micropaleontology 51, 129–152.
Scourse, J., Trouet, V., Raible, C., 2010. The Medieval Climate Anomaly and the Little Ice Age: testing the NAO hypothesis. In "EGU." Geophysical Research Abstracts, Vienna.
Shackleton, N., 1974. Attainment of isotopic equilibrium between ocean water and the benthonic foraminifera genus Uvigerina: isotopic changes in the ocean during the last glacial. Colloq. Int. C.N.R.S. 219, 203–209.
Shindell, D.T., Schmidt, G.A., Mann, M.E., Rind, D., Waple, A., 2001a. Solar forcing of regional climate change during the Maunder Minimum. Sci. 294, 2149–2151.
Shindell, D.T., Schmidt, G.A., Miller, R.L., Rind, D., 2001b. Northern Hemisphere winter climate response to greenhouse gas, ozone, solar and volcanic forcing. Journal of Geophysical Research 106, 7193–7210.
Sicre, M.-A., Jacob, J., Ezat, U., Rousse, S., Kissel, C., Yiou, P., Eiríksson, J., Knudsen, K.L., Jansen, E., Turon, J.-L., 2008. Decadal variability of sea surface temperatures off North Iceland over the last 2000 years. Earth and Planetary Science Letters 268, 137–142.
Steinhilber, F., Beer, J., Fröhlich, C., 2009. Total solar irradiance during the Holocene. Geophsical Res. Lett. 36.
Stuiver, M., Reimer, P.J., 1993. Extended $^{14}C$ data-base and revised calib 3.0 $^{14}C$ age calibration program. Radiocarbon 35, 215–230.
Stuiver, M., Reimer, P.J., Braziunas, T.F., 1998. High precision radiocarbon age calibration for terrestrial and marine samples. Radiocarbon 40, 1127–1151.
Sturges, W., Hong, B.G., Clarke, A.J., 1998. Decadal Wind Forcing of the North Atlantic Subtropical Gyre. Journal of Physical Oceanography 28, 659–668.
Swart, P.K., Greer, L., Rosenheim, B.E., Moses, C.S., Waite, A.J., Winter, A., Dodge, R.E., Helmle, K., 2010. The 13C Suess effect in scleractinian corals mirror changes in the anthropogenic CO2 inventory of the surface oceans. Geophysical Research Letters 37, L05604.
Swingedouw, D., Terray, L., Cassou, C., Voldoire, A., Salas-Mélia, D., Servonnat, J., 2010. Natural forcing of climate during the last millennium: fingerprint of solar variability. Climate Dynamics 36, 1349–1364.
Tachikawa, K., Elderfield, H., 2002. Microhabitat effects on Cd/Ca and δ13C of benthic foraminifera. Earth and Planetary Science Letters 202, 607–624.
Thornalley, D.J.R., Elderfield, H., McCave, I.N., 2009. Holocene oscillations in temperature and salinity of the surface subpolar North Atlantic. Nature 457, 711–714.
Tomczak, M., Godfrey, J.S., 1994. Reg. Oceanography. Pergamon, Oxford.
Trouet, V., Esper, J., Graham, N.E., Baker, A., Scourse, J.D., Frank, D.C., 2009. Persistent positive North Atlantic Oscillation Mode dominated the Medieval Climate Anomaly. Science 324, 78–80.
Villanueva Guimerans, P., Cervera Currado, J.L., 1999. Distribution of Planorbulinacea (benthic Foraminifera) assemblages in surface sediments on the northern margin of the Gulf of Cadiz. Boletin. Instuto Espanol de Oceanografia 15, 181–190.
Wilson, P., McGourty, J., Bateman, M.D., 2004. Mid-to late-Holocene coastal dune event stratigraphy for the north coast of Northern Ireland. Holocene 14, 406–416.
Wintle, A.G., Clarke, M.L., Musson, F.M., Orford, J.D., Devoy, R.J.N., 1998. Luminescence dating of recent dunes on Inch Spit, Dingle Bay, southwest Ireland. Holocene 8, 331–339.
Xue, Y.T.M., Smith, T.M., Reynolds, R.W., 2003. Interdecadal changes of 30-yr SST normals during 1871–2000. J. of Climate 16, 1601–1612.